


Field Investigations of the Geometric Features of Wind Wave Breaking

A. E. Korinenko , V. V. Malinovsky

Marine Hydrophysical Institute of RAS, Sevastopol, Russian Federation

 *korinenko.alex@mhi-ras.ru*

Abstract

Purpose. The paper is purposed at studying temporal variability of the geometric dimensions of wind wave breaking under natural conditions and at assessing the fraction of the sea surface covered with foam using the distribution of the breaking wave crest lengths.

Methods and Results. Field studies of the wave breaking characteristics were carried out from the stationary oceanographic platform located at 500 m off the Katsiveli coast (Black Sea hydrophysical subsatellite polygon). Geometric dimensions of wave breaking in the active phase and the velocity of wave movement were determined using video records of sea surface. Processing of video frame sequences has resulted in formation of the array of crest lengths, and the array of widths and areas of the varying in time foam structures. Meteorological information was obtained simultaneously with video records.

Conclusions. A connection independent of wind and wave conditions was established experimentally between the wave breaking geometric dimensions and the breaking wave length: the average width of breaking is proportional to the length of a breaking wave, the average area – to the squared length of a carrier wave. The values of these ratios are 0.03 and 0.002, respectively, that confirms the geometric similarity of wave breaking. It is shown that the length and width of an individual wave breaking increase at a constant rate, the value of which is conditioned by the scale of a breaking wave. The geometric characteristics of wave breaking normalized to the length of a breaking wave are linearly dependent on dimensionless time and independent of the scales and velocities of breaking waves. To calculate the fraction of sea surface covered with foam, the distributions of the wave breaking lengths were used. The field data values are shown to be adequately corresponding to the calculations by the model proposed by O. M. Phillips.

Keywords: wind wave breaking, field studies, distribution of breaking lengths, breaking similarity, fraction of the sea surface covered with wave breaking foam, growth rate of linear dimensions of breaking

Acknowledgements: The study was financially supported by the Russian Science Foundation grant No. 21-17-00236, <https://rscf.ru/project/21-17-00236/>. The study involved the archival data obtained within the framework of the theme of state assignment FNNN-2021-0004 “Fundamental research of oceanological processes that determine state and evolution of the marine environment under the influence of natural and anthropogenic factors, based on observation and modeling methods”.

For citation: Korinenko, A.E. and Malinovsky, V.V., 2023. Field Investigations of the Geometric Features of Wind Wave Breaking. *Physical Oceanography*, 30(6), pp. 776-791.

© 2023, A. E. Korinenko, V. V. Malinovsky

© 2023, Physical Oceanography

Introduction

Wave breaking at the sea surface is a complex hydrodynamic phenomenon. During its evolution, the foam structure goes through a whole range of intermediate states – from a breaker with a foaming crest to a disintegrating emulsion layer. According to [1, 2], two classes of foam formations can be fairly confidently



identified in optical images of the sea surface: crests (whitecaps, active phase) and spotty structures (residual foam, passive phase).

The study of various properties of foam structures enables us to make certain simplifications in numerical models or draw conclusions about the possible causes of certain physical processes. For example, in the phenomena of gas exchange and intrinsic microwave radiation of the sea surface, the passive phase is most important [3]. A detailed description of statistical and geometric characteristics of foam structures in the active phase is necessary for calculating wave energy dissipation of gravity waves during their breaking [4, 5] and developing remote sensing methods for studying the sea surface [3, 6, 7].

In this work, based on optical recording of the sea surface, the emphasis is made on studying the whitecap dimension evolution.

In one of the first laboratory works [4] devoted to the study of kinematic characteristics of quasi-stationary breakings, it was found that this type of breaking is geometrically similar. In [4], a linear relationship between geometric dimensions of breaking and the breaking wave length λ was established. In this work, the research has shown that the rate of wave energy dissipation as a result of breaking is proportional to the fifth power of the whitecap speed and depends on its geometry. Experiments in open sea conditions [8, 9] confirmed that whitecaps are geometrically similar. The ratio of average length of the whitecap crest L to the breaking wave length and the ratio of a whitecap lifetime to the carrier wave period do not depend on hydrometeorological observation conditions and breaking scale. In [10, 11], an analysis of geometric dimensions of individual foam structures was performed and it was demonstrated that wave breakings have stable geometric ellipsoidal shape with an eccentricity of 0.98 [11], which was practically independent of wind conditions.

However, when using average whitecap characteristics obtained under natural conditions, it is difficult to estimate directly the constant connecting the wave energy dissipation with the distribution of breaking lengths [4].

In [12], a model is proposed to calculate wave energy dissipation due to breaking, which uses time evolution of the foam structure area. Information about changes in the geometric characteristics of breaking over time is required for the development of models of the radar scattering non-Bragg component [13, 14].

Despite the obvious need to study the evolution of individual whitecap dimensions and their variability under various hydrometeorological parameters, the amount of research in this area is insufficient.

The work aims to study the relationship between breaking wave parameters and time-varying geometric characteristics of whitecaps for the development of wave models and improvement of remote methods for diagnosing marine environment.

Experiment

In this work, we used a database of archival data obtained during the autumn periods of 2015, 2018 and 2019 when performing field experiments at a stationary oceanographic platform in the Goluboy Gulf near Katsiveli (Black Sea hydrophysical subsatellite polygon, the Southern Coast of Crimea). The platform is installed approximately 500 m off the shore.

The process of recording wind wave breaking using a video camera is described in [8]. The video camera we used, with a lens providing horizontal viewing angles of 54° and vertical ones of 32° , recorded at a frequency of $f_{\text{rec}} = 25$ frames per second and a resolution of 1920×1080 pixels. The camera was installed on the deck of the platform at 11.4 m height above the sea level with a viewing direction of 30° – 40° to the horizon and 50° – 60° to the “windward” direction.

Wind speed and direction were measured by Davis 6152EU complex, which includes a meter for these parameters, an air temperature sensor and a water temperature sensor installed at a 3-m depth. An anemometer was located on the oceanographic platform mast at 23 m above the sea level. Its data was recalculated into the effective neutrally stratified wind velocity U at 10 m according to the method [15].

The field data were obtained with neutral atmosphere stratification and wind velocities of 8–21 m/s.

Data processing technique. To determine various characteristics of an active phase of breaking, the technique [16] was applied. Let us list the main processing stages required in this work. The algorithm for identifying breakings from the sea surface video recordings is based on comparing the Gaussian distribution of brightness $p(I)$ within a video frame in the absence of breakings and the real distribution $p(I')$ with regard to foam structures. The presence of breakings distorts the Gaussian distribution shape significantly and increases $p(I')$ relative to $p(I)$ at brightness exceeding the threshold value I_0 . When $I > I_0$, a sea surface section in the video frame is considered as a foam structure [16].

Further data processing consists of isolating the active phase of breakings and ignoring the spreading foam remaining after the whitecap passage. At this stage, the kinematic properties of breakings in various phases are used. When analyzing the kinematic characteristics of breaking, it is assumed that in the active phase a whitecap moves at a constant velocity and reaches maximum area values at $t = \tau$ (see, for example, [16–18]).

At the final stage of data processing, the image frame was tied to coordinates on a horizontal plane located at mean sea level taking into account the observation geometry. Depending on the shooting geometry, the spatial resolution was $\sim 1 \dots \sim 2.5$ cm. The dimensions of a whitecap were determined in each frame: length L and crest width l , occupied area S , coordinates of the whitecap geometric center (x_c, y_c) . To determine L and l , the coordinates of the whitecap outer boundary were found. The length L was calculated as the maximum distance between the points of the resulting contour. The crest width l was defined as a segment perpendicular to L , passing through the whitecap geometric center.

For each individual breaking, during its lifetime τ in the active phase, a group of consecutive video frames with a time interval $\Delta t = 1/f_{\text{rec}}$ s between them was formed. At the same time, for the first frame in the selected group the time was set as $t = 0$. This provided the study of time evolution patterns of individual breaking characteristics.

An example of determining the main geometric dimensions of wave breaking is demonstrated in Fig. 1. The modulus of breaking velocity was determined as

$c = \sqrt{(c_c^x)^2 + (c_c^y)^2}$ and movement direction as $\varphi_{wb} = \arctg(c_c^y/c_c^x)$, where $c_c^x = \partial x_c/\partial t$ and $c_c^y = \partial y_c/\partial t$ are the velocity components.

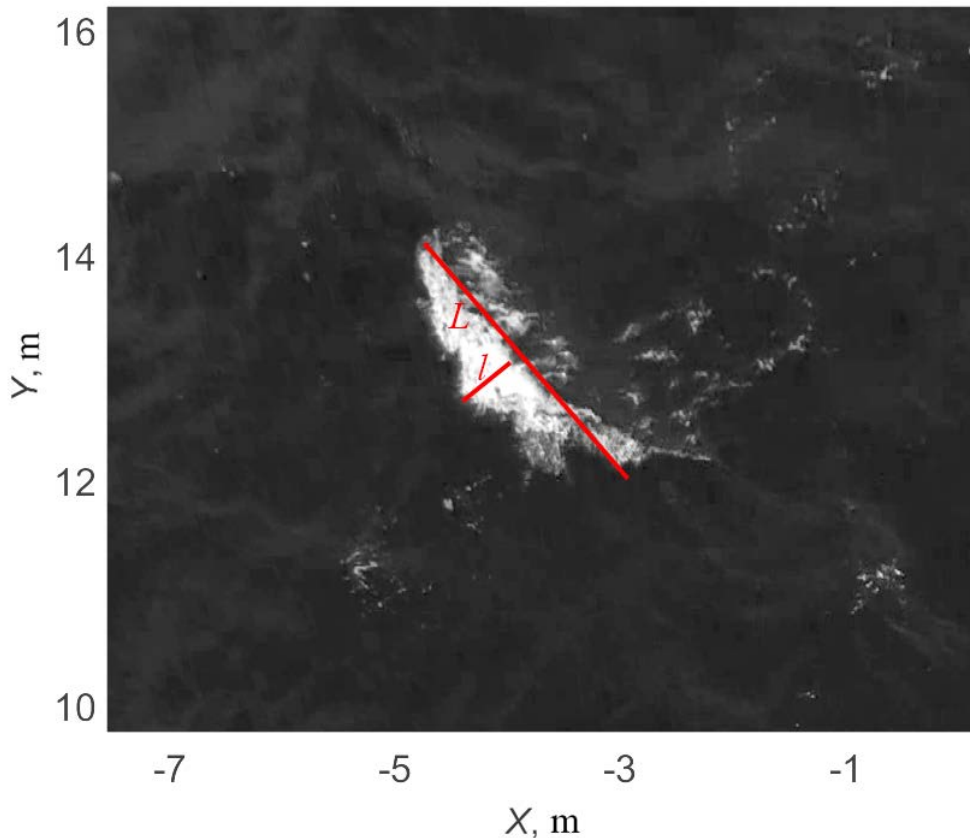


Fig. 1. Fragment of the image linked to the coordinates on the horizontal plane (L is whitecap length, l is its width)

In accordance with [5], in this work we assume that the breaking velocity is equal to the phase velocity of breaking wave. Then, taking into account the dispersion relation, the breaking wave length can be determined as $\lambda = gc^2/2\pi$, where g is gravitational acceleration.

Some elements of data processing procedure are shown in Fig. 2 and Fig. 3. Fig. 2 presents a series of 6 sea surface images, where one can trace the main stages of evolution of an individual foam formation (indicated by a dotted line). Red color indicates sea surface areas which are identified as the active phase of breaking by the algorithm [16]; the residual foam is marked in yellow. At the initial stage of the foam structure evolution, the whitecap is rigidly connected with the breaking wave and therefore moves with its phase velocity [5]. As can be seen from Fig. 2, $a - d$, the foam zone significantly increases in size and moves away from the initial section of the sea surface where it was formed.

Spots of residual foam eventually begin to separate from the foam structure moving as a single unit. At this stage, the foam zone has a mixed form, i.e. the ending active phase and forming residual foam (Fig. 2, *d*). Here, the active phase and residual foam are indistinguishable in visible images. Then there is a decrease in the foam zone area and the passive phase acquires a clearly expressed scattered spotty structure. In the last two frames of Fig. 2, *e, f*, the residual foam structure, located near the lower boundary of the image, is clearly visible.

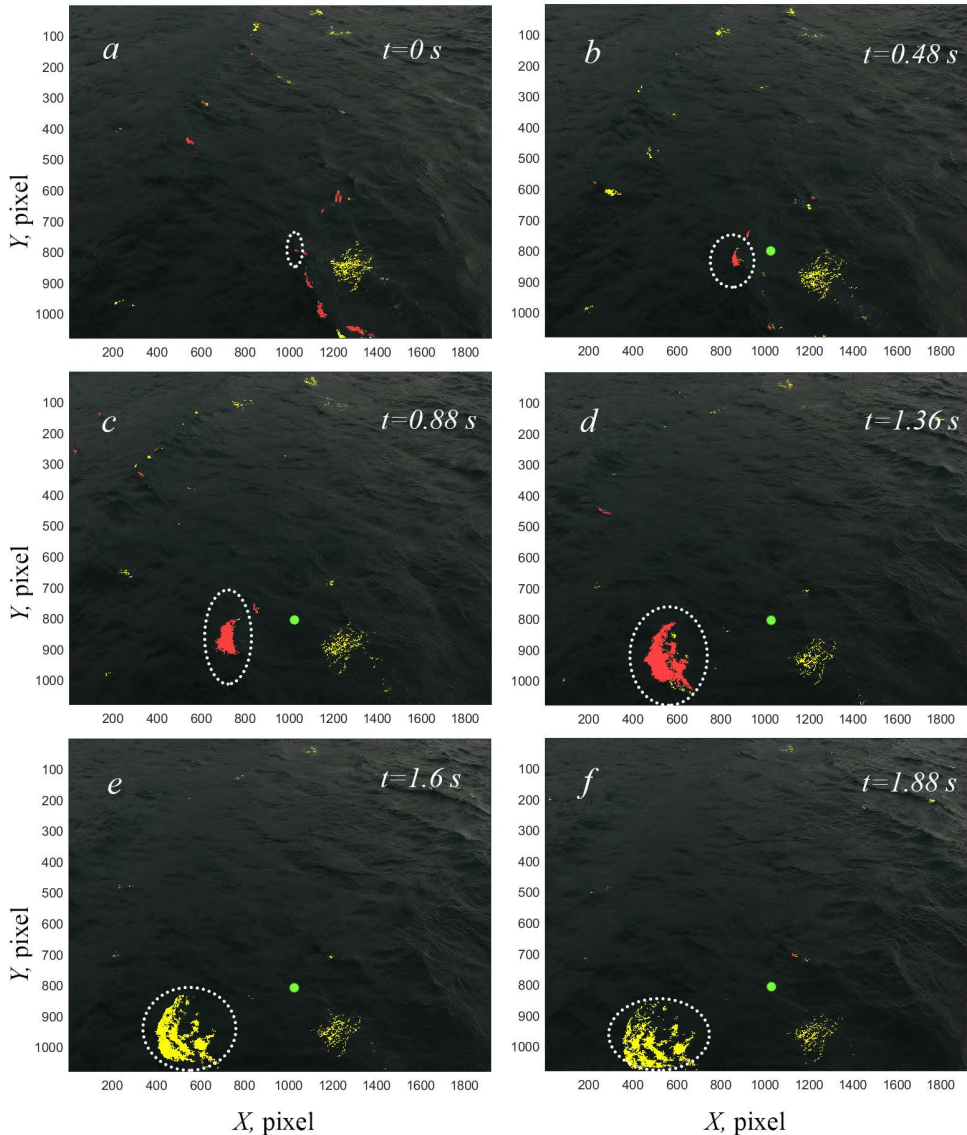


Fig. 2. Evolution of foam structure: *a* – whitecap formation; *b* – *d* – movement and growth of foam structure dimensions; *e, f* – spot of spreading foam after the whitecap disappearance. Green dot marks the sea surface area where the whitecap was first identified

Fig. 3 shows the characteristic timing cycle of the area, crest length and coordinates of the geometric breaking center. Vertical straight lines sequentially correspond to the frames given in Fig. 2. As follows from Fig. 3, *a*, the foam zone increases at the initial stage and starts to decrease at the moment t_4 , which indicates the end of the active phase, and at $t > t_4$ the residual foam starts to make a predominant contribution to the foam structure formation.

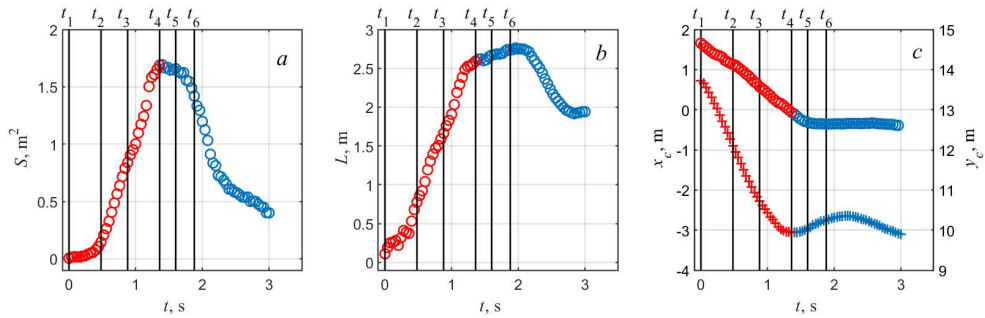


Fig. 3. Evolution of wave breaking geometric dimensions (highlighted by a dotted line in Fig. 2): *a* – area; *b* – crest length; *c* – coordinates of geometric center of whitecap x_c and y_c . Active phase of wave breaking is shown in red

The difference of residual foam dynamics from the active phase can also be seen from the temporal evolution of the position of centroid coordinates in Fig. 3, *c*. The whitecap moves at a constant velocity (red symbols (+) and (o) for x_c and y_c respectively), while the motion of the residual foam geometric center begins to oscillate reflecting orbital movements of dominant waves. Thus, the determination of the active phase of breaking relied on the constancy of geometric center velocity modulus and the increase of the whitecap area. After reaching the maximum breaking area, we assume that the foam structure passes from the active phase to the passive one.

Additional information about the algorithm and calculation of various characteristics of wind wave breaking is given in [8, 16]. This work considers only those whitecaps that arose and broke within the observed region.

Results and data analysis

Relationship between the geometric dimensions of breaking and the parameters of breaking waves. The resulting database, which contains information about the breaking dimensions and breaking wave scale, enables us to associate the whitecap average dimensions with λ .

Let us consider the dependence of the whitecap minor axis and its area on λ . The range of breaking wave lengths 3.7–18.7 m was divided into 5 intervals with a step $\Delta\lambda = 3$ m. In each of the ranges $(\lambda, \lambda + \Delta\lambda)$, the average value of \bar{l} and \bar{S} was determined and the value of the breaking wave length corresponded to the middle of $(\lambda, \lambda + \Delta\lambda)$ interval.

In Fig. 4 the dependence of \bar{l} and \bar{S} upon λ is demonstrated. The lines there correspond to the dependences $\bar{l} = (0.028 \pm 0.001)\lambda$ and $\bar{S} = (0.0021 \pm 0.0002)\lambda^2$, where the coefficients are obtained by the least squares method. Vertical segments indicate standard deviations $\pm\delta l$ and $\pm\delta S$ for the values \bar{l} and \bar{S} located within the corresponding interval $(\lambda, \lambda + \Delta\lambda)$.

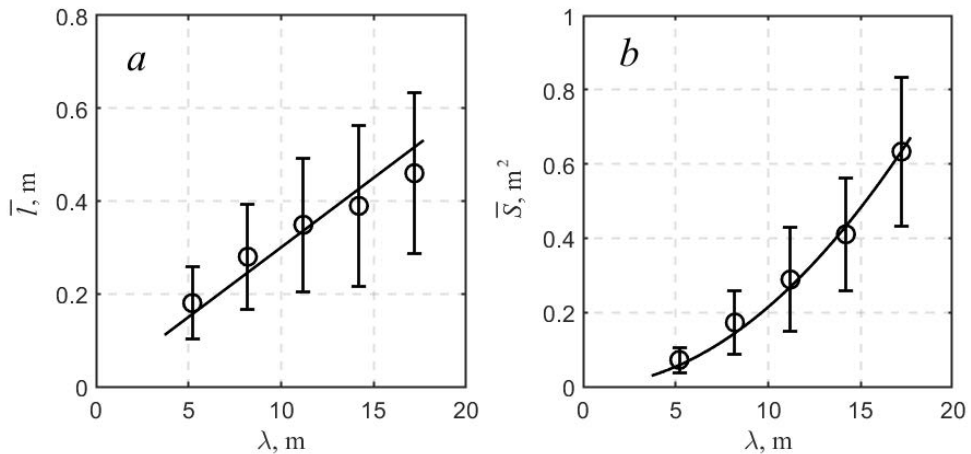


Fig. 4. Dependence of the minor axis (a) and the area (b) of a whitecap in the active phase upon the breaking wave length

The obtained expressions relating average values of breaking width and area with the breaking wave length are of undoubted interest, since their dependencies imply $\bar{l}/\lambda \cong 0.03$ and $\bar{S}/\lambda^2 \cong 0.002$. Considering the fact that in the active phase the ratios $\bar{L}/\lambda \cong 0.1$ [8] and $\bar{\tau}/T \cong 0.33$ [9] are also constant and independent of hydrometeorological observation conditions and breaking scale, we can talk about self-similarity of linear dimensions of breakings, their areas and lifetime.

Estimation of growth rate of whitecap geometric dimensions. When analyzing experimental data on breakings, their maximum and average lengths, areas and lifetimes are mainly assessed. Temporal variability of geometric dimensions L , l , S of individual whitecaps remains practically unstudied. At the same time, the form of dependences $L(t)$, $l(t)$ and $S(t)$ can be of undoubted interest in problems of studying wave dynamics and developing radar scattering models [12–14].

Evolution of the foam zone geometric dimensions in the active phase is considered below. We divide the range of the whitecap movement velocity (2.4–5.4 m/s) into 5 intervals with a step of $\Delta c = 0.6$ m/s and find the average value of $L^m(t)$, $l^m(t)$ and $S^m(t)$ in each considered velocity range. Note that the moment t was determined relative to the beginning of each breaking and for a fixed t value of all whitecap lengths and areas averaged in a given velocity interval.

Temporal evolution of the whitecap kinematic characteristics $L^m(t)$, $l^m(t)$ and $S^m(t)$ for each of the selected velocity ranges $(c, c + \Delta c)$ is presented in Fig. 5. For better visualization, variation intervals of breaking lengths and areas values for each range $(c, c + \Delta c)$ are shown in colored areas. The upper and lower boundaries

of the zones are defined as $L^m(t) \pm \delta L^m(t)$, $l^m(t) \pm \delta l^m(t)$ and $S^m(t) \pm \delta S^m(t)$, where $\delta L^m(t)$, $\delta l^m(t)$, $\delta S^m(t)$ are root-mean-square deviations of random values of breaking lengths and areas at t moment. The dependences L^m and l^m in Fig. 5, a , b are close to linear, while S^m is close to power law dependence. From Fig. 5 it follows that the greater the breaking wave velocity and, consequently, its scale, the faster the whitecap geometric dimensions increase.

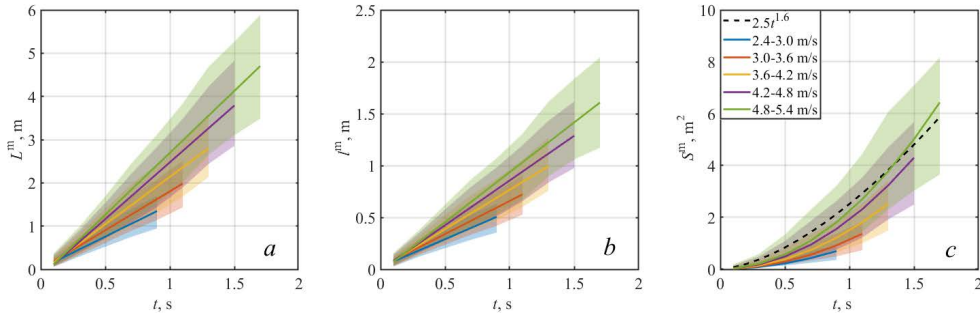


Fig. 5. Temporal dependence of the whitecap geometric dimensions: a – length along the crest; b – width; c – area (solid colored lines denote parameterizations $L^m(t)$, $l^m(t)$ and $S^m(t)$; the velocity range ($c, c + \Delta c$)) is shown in color

We approximate the breaking length and width variation using linear dependencies:

$$\begin{aligned} L^m(t) &= a^L t, \\ l^m(t) &= a^l t, \end{aligned} \quad (1)$$

where a^L , a^l coefficients were obtained by the least squares method and indicate the growth rate of the whitecap length and width in the active phase.

The temporal variability S^m deserves a separate discussion. For all intervals ($c, c + \Delta c$), the dependence of breaking areas on t is described well by the power function $S^m(t) = a^S t^q$, where q varies from a minimum value of 1.4 to a maximum of 1.6 in the first and fifth range of breaking velocities, respectively. In Fig. 5, c , for example, the dashed line indicates the approximation $S^m(t) = 2.5t^{1.6}$ obtained for $c \in (4.8-5.4 \text{ m/s})$.

At the same time, one would expect that the area of the figure that describes breaking is determined by the product of the axes (equation (1)). In this case, the temporal variation of the whitecap area should have a quadratic dependence $S^m(t) \propto a^L a^l t^2$. In a number of studies, when determining the breaking characteristics from optical images, the whitecap boundaries are approximated by an ellipse [10, 11, 19, 20]. If we assume that the foam structure shape in the active phase is close to an ellipse, then, according to equation (1), the area of a single breaking will be written as follows:

$$S^m(t) = a^S t^2, \quad (2)$$

where $a^S = \pi a^L a^l / 4$.

The difference of q power values we obtained from 2 in temporal dependences $S^m(t)$ requires a separate discussion. From our point of view, such a difference in degrees may be due to the fact that the termination moment of the active phase of

breaking is determined at $t = t_4$ (Fig. 3, *a*), when the value of the whitecap area reaches its maximum. At the same time, a mixed phase appears in the interval $t_3 < t \leq t_4$; during this time period the residual foam begins to separate from the whitecap (Fig. 2, *d*). As a result, the growth rate of breaking area decreases and at $t = t_4$ it becomes equal to zero, $\partial S^m(t)/\partial t|_{t=t_4} = 0$. The underestimated values of q powers in our case are due to the fact that the dependences $S^m(t)$ were approximated over the entire interval of the active phase of breaking $0 \leq t \leq t_4$, including the zone in the vicinity of the maximum area, where its variation rate is significantly lower and reaches zero.

Analysis of the data we obtained reveals that in the absence of a mixed phase in the interval $0 \leq t \leq (t_3 + t_4)/2$, the temporal variation of breaking area is satisfactorily described by the quadratic dependence (1). The study of temporal variability of the whitecap parameters in the transition phase requires more detailed additional research and is beyond the scope of this work.

Here, we are to describe temporal dependence of the whitecap area with the help of expression (2). Fig. 5 shows solid-colored lines denoting functions $S^m(t) = a^S t^2$ for selected velocity ranges.

The dependence of the obtained coefficients a^L , a^l and a^S on the average breaking velocity in the intervals $(c, c + \Delta c)$ is shown in Fig. 6, where the vertical segments correspond to the values of root-mean-square deviations $\pm \delta a^L$, $\pm \delta a^l$, $\pm \delta a^S$. The lines denote the dependences calculated by the least squares method: $a^L = (0.56 \pm 0.04)c$, $a^l = (0.19 \pm 0.01)c$, $a^S = (0.09 \pm 0.01)c^2$.

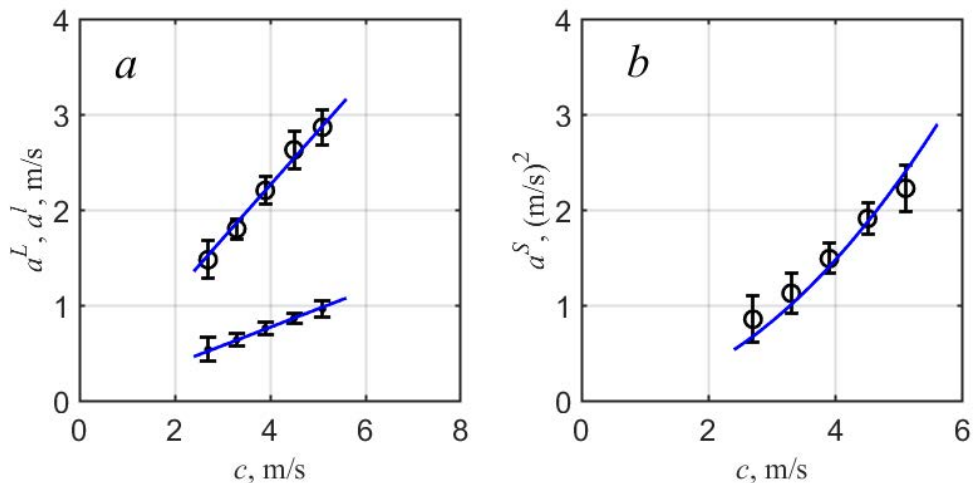


Fig. 6. Dependences a^L , a^l (*a*) and a^S (*b*) on the breaking wave velocity

The dependence of the obtained coefficients a^L , a^l and a^S on the average breaking velocity in the intervals $(c, c + \Delta c)$ is demonstrated in Fig. 6, where the vertical segments correspond to the values of root-mean-square deviations $\pm \delta a^L$, $\pm \delta a^l$, $\pm \delta a^S$. The lines denote the dependences $a^L = (0.56 \pm 0.04)c$, $a^l = (0.19 \pm 0.01)c$ and $a^S = (0.09 \pm 0.01)c^2$ calculated by the least squares method.

Considering the obtained functional dependencies of a^L , a^l , a^S coefficients, expressions (1) and (2) will be written in the following form:

$$\begin{aligned} L(t) &= (0.56 \pm 0.04)ct, \\ l(t) &= (0.19 \pm 0.01)ct, \end{aligned} \quad (3a)$$

$$S(t) = (0.09 \pm 0.01)c^2t^2. \quad (3b)$$

As the field data analysis showed, the whitecap linear dimensions increase at a constant rate, the value of which is determined by the breaking wave scale. At the same time, the whitecap area increases with time according to quadratic law and the growth rate S is proportional to c^2 .

We introduce dimensionless values $L'(t') = L(t)/\lambda$, $l'(t') = l(t)/\lambda$, $S'(t') = S(t)/\lambda^2$, $t' = t/T$. Then expressions (3a) and (3b), with account for the obvious relation $c = \lambda/T$, can be written down as

$$\begin{aligned} L'(t') &= 0.6t', \\ l'(t') &= 0.2t', \end{aligned} \quad (4a)$$

$$S'(t') = 0.1(t')^2. \quad (4b)$$

It follows from expressions (4) that evolution of the whitecap dimensionless geometric magnitudes in the active phase does not depend on the scale of the breaking waves.

The verification of the last statement is of interest. Indeed, semi-empirical dependences (4) were obtained for all values of c . We are to consider how significant the differences in the functions in formulas (4) will be at different velocities of breaking movement. Fig. 7 presents the variations by t' of the dimensionless length, crest width and dimensionless area of the whitecaps lying in the above-mentioned intervals ($c, c + \Delta c$). Solid lines in Fig. 7, $a - c$ indicate the dependences $L'(t') = a^{L'}t'$, $l'(t') = a^{l'}t'$, $S'(t') = a^{S'}(t')^2$ respectively, where the values of $a^{L'}$, $a^{l'}$, $a^{S'}$ coefficients were obtained by the least squares method. The color of the lines corresponds to the velocity range ($c, c + \Delta c$) (see explanatory notes). The colored areas in Fig. 7 show the areas where the values $L'(t') \pm \delta L'(t')$, $l'(t') \pm \delta l'(t')$ and $S'(t') \pm \delta S'(t')$ respectively, are located.

As follows from Fig. 7, a, b , the data $L'(t')$ and $l'(t')$ are grouped into dependences which are close to linear ones, with slopes of ~ 0.6 and ~ 0.2 , respectively, for all values of the breaking wave velocity, which is consistent with the coefficients in formula (4a). Dependences of breaking areas on dimensionless time for selected c , demonstrated in Fig. 7, c , are also close and group around $S'(t') = 0.1(t')^2$, which coincides with expression (4b).

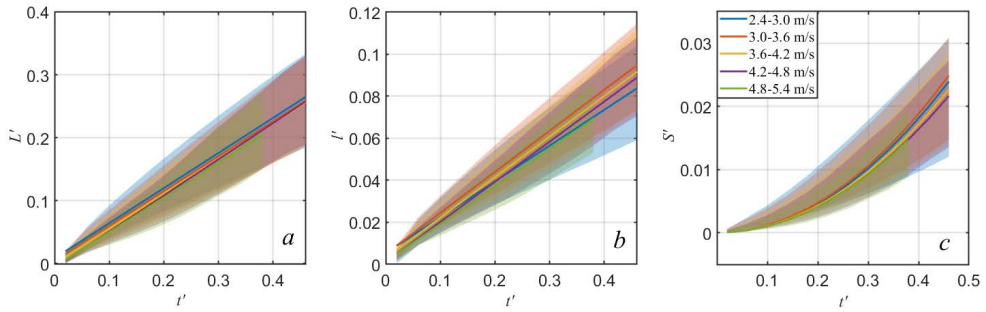


Fig. 7. Dependence of the dimensionless length (*a*), width (*b*) and area (*c*) on the dimensionless time. Solid lines correspond to the dependences obtained in the velocity intervals indicated in the legend

Fraction of foam-covered sea surface as a function of breaking length distribution. The fraction of the sea surface covered with breaking wave foam, W , is one of the main indicators of the dynamic processes of atmosphere – ocean interaction. In [5], it was proposed to use the distribution of wave crest lengths $\Lambda(\mathbf{c})$ as a statistical measure of wave breaking. The integral $\int \Lambda(\mathbf{c}) d\mathbf{c}$ is equal to the total length of the breaking crests per unit area of the sea surface. According to [5], at the moment of a whitecap generation, a foam zone appears which is formed by the moving breaking front and stays throughout the entire τ_p lifetime; in this case the total fraction of the foam-covered sea surface is written as

$$W = \int c\tau_p\Lambda(\mathbf{c})d\mathbf{c}. \quad (5)$$

On the other hand, when carrying out field studies, the breaking area S is recorded. When moving and increasing in dimensions, the whitecap does not leave visible bubbles behind and, as follows from Fig. 2, *a – d*, the surface behind the breaking is free of residual foam during the active phase. Then we should expect that the fraction of the sea surface W_E occupied by whitecaps will be less than W calculated by equation (5). We write down this equation for the fraction of the foam-covered sea surface in the active phase in the following form:

$$W_A = c_a \int c\tau\Lambda(\mathbf{c})d\mathbf{c}, \quad (6)$$

where c_a is a coefficient indicating that the foam zone area in the active phase is less than the total foam content of the sea surface ($\tau_p = \tau$ for the active phase). The justification for calculating W_A using expression (6) is presented in the Appendix. When calculating the non-Bragg scattering component in [7, 13], an expression similar to formula (6) was applied; c_a coefficient in these works was estimated by the correspondence of model calculations of the non-Bragg scattering component to field data.

Let us compare W_E values measured in the experiment and W_A calculated by formula (6) on the basis of the same database. W_E values were determined as

the average area of recorded breakings per unit of sea surface, which is a traditional method applied in numerous experimental studies:

$$W_E = \sum_i S_i / (AN_{fr}),$$

where A is a viewing area of the sea surface; N_{fr} is number of video frames. The duration of video recordings from which W_E was calculated varied within 20–30 min range.

The calculation of W_A values using field data was carried out as follows. According to the results of our measurements, one-dimensional distribution $\Lambda(c)$ was estimated as $\Lambda(c) = \frac{1}{A \cdot \Delta c \cdot N_{fr}} \sum_k L_k |c_k \in [c, c + \Delta c]$, where Δc is the velocity interval, in our case equal to 0.5 m/s; L_k is the length of the k -th crest of breaking wave moving at c_k velocity within the interval $c_k \in (c, c + \Delta c)$.

According to [9, 21], $\tau = \gamma_\tau T$, where γ_τ is proportionality coefficient; $T = \frac{2\pi}{g} c$ is breaking wave period. Based on the foregoing, we write down expression (6) for W_A in the following form:

$$W_A = c_a \frac{2\pi\gamma_\tau}{g} \int c^2 \Lambda(c) dc. \quad (7)$$

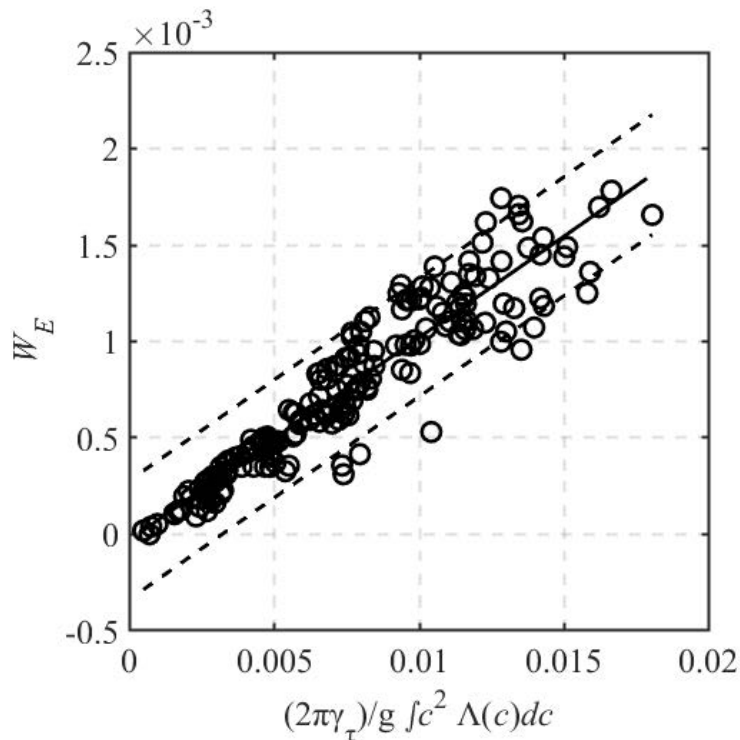


Fig. 8. Fraction of the sea surface covered with foam of breaking waves as compared to $\frac{2\pi\gamma_\tau}{g} \int c^2 \Lambda(c) dc$ (solid line is the data approximation by linear dependence, dashed lines are 95% confidence intervals)

Now we are to estimate the value of c_a coefficient. Fig. 8 gives a comparison of W_E and $\frac{2\pi\gamma_\tau}{g} \int c^2 \Lambda(c) dc$, where in accordance with [9] $\gamma_\tau = 0.33$; a solid line indicates the dependence $W_E = c_a \frac{2\pi\gamma_\tau}{g} \int c^2 \Lambda(c) dc$, where the value $c_a = 0.11 \pm 0.01$ was obtained by the least squares method.

Thus, expression (5) can be used with regard to the correction factor c_a in the models, when calculating the fraction of the sea surface covered by breakings in the active phase.

Conclusion

The work presents the results of field studies of temporal evolution patterns of geometric characteristics of gravitational wave breaking. Determination of breaking dimensions in the active phase and velocity of their movement was carried out using video recordings of the sea surface.

It has been experimentally shown that the average values of the whitecap width are linearly related to the breaking wave length $\bar{l} = 0.03\lambda$ and average areas of breakings are proportional to the square of the breaking wave length $\bar{S} = 0.002\lambda^2$. The relationships we found complement the results obtained earlier by the authors ($\bar{L}/\lambda \cong 0.1$ and $\bar{\tau}/T = 0.33$). Based on the experimentally obtained relationships for the crest lengths, minor axes, areas and lifetime in the active phase of breaking, which are constants, a conclusion on the geometric and kinematic similarity of breakings was drawn.

It has been experimentally shown that geometric dimensions of an individual whitecap (length and width) grow at constant rates and their values are determined by c : $a^L = (0.56 \pm 0.04)c$, $a^l = (0.19 \pm 0.01)c$. A quadratic dependence of growth of an individual breaking area on time has been established and the value of the leading coefficient is determined as $a^S = (0.09 \pm 0.01)c^2$.

The values of crest lengths and breaking widths normalized to the breaking wave length linearly depend on the dimensionless time $t' = t/T$, practically coincide and are grouped around the universal dependencies $L(t)/\lambda \cong 0.6t'$ and $l(t)/\lambda \cong 0.2t'$. The dependences of the areas normalized to λ^2 on t' are also close and grouped around $S(t')/\lambda^2 = 0.1(t')^2$. The obtained results enable us to speak about the independence of dimensionless geometric characteristics of breaking from breaking wave scale and velocities.

Calculations of the sea surface fraction covered with the foam of breaking waves were performed both in the traditional way (the average area of recorded breakings per unit of sea surface was calculated) and using statistics on the distribution of the breaking crest lengths.

A comparison of W_E with W values calculated using expression (7) showed a linear dependence $W_E = c_a \frac{2\pi\gamma_\tau}{g} \int c^2 \Lambda(c) dc$, where $c_a = 0.11 \pm 0.01$. Thus, one can use the expression for W proposed by O.M. Phillips, $W_E = c_a W$, in the developed models for describing sea surface. Taking into account the experimental estimates of a^l and γ_τ parameters obtained in this work, an explanation for the value of c_a coefficient is proposed.

Appendix

To estimate the model values of the sea surface fraction covered with active-phase breakings, we use the concept of $\Lambda(c)$ function proposed in [5]. Now we move on to a coordinate system with the origin at the foam structure center. We write down the variation of a single whitecap area over time dt as follows:

$$dS \cong dLdl, \tag{A1}$$

where dL , dl are increments in the breaking dimensions. According to expressions (1) and (2), $dL = a^l dt$, $dl = a^l dt$, and integrating equation (A1) over the breaking lifetime, we obtain an expression for the maximum whitecap area

$$S_m \cong a^l \tau L_m, \tag{A2}$$

where $L_m = a^l \tau$ is maximum length of breaking crest. Since, as shown above, $L(t)$ increases linearly from 0 to L_m , the average crest length is $\bar{L} = L_m/2$. According to the data in Fig. 5, c , $S(t)$ is described by a quadratic temporal dependence, and as a result, the ratio of the maximum area to its average value will be $\frac{S_m}{\bar{S}} = 3$. Using the relationships given here for the breaking lengths and areas, we rewrite expression (A2) for the average area of a single whitecap:

$$\bar{S} \simeq \frac{2}{3} a^l \tau \bar{L}. \tag{A3}$$

Summing up expressions (A3) for all breakings observed in area A , we obtain

$$\frac{1}{A} \sum_i \bar{S}_i \simeq \frac{2}{3A} a^l \tau \sum_i \bar{L}_i. \tag{A4}$$

Considering the fact that total breaking length per unit surface is $\int \Lambda(c) dc = \frac{1}{A} \sum_i \bar{L}_i$, and the left side in expression (A4) is the fraction of the sea surface W_A covered by the active phase of breaking waves, we rewrite expression (A4) in the following form:

$$W_A = 2/3 \int a^l \tau \Lambda(c) dc. \tag{A5}$$

The main difference between formula (A5) and equation (5) is that in the integrand (A5) the factor is not the whitecap movement velocity, but the growth rate of its minor axis a^l . According to the results presented above, $a^l = 0.2c$. Then

$$W_A = c'_a \frac{2\pi\gamma\tau}{g} \int c^2 \Lambda(c) dc,$$

where $c'_a = \frac{2}{3} 0.2 = 0.13$. The expression exactly coincides with formula (7), while c'_a and c_a values are close.

REFERENCES

1. Bondur, V.G. and Sharkov E.A., 1982. Statistical Characteristics of Foam Formations on a Disturbed Sea Surface. *Oceanology*, 22(3), pp. 372-379 (in Russian).
2. Monahan, E.C. and Woolf, D.K., 1989. Comments on "Variations of Whitecap Coverage with Wind Stress and Water Temperature". *Journal of Physical Oceanography*, 19(5), pp. 706-709. doi:10.1175/1520-0485(1989)019<0706:COOWCW>2.0.CO;2
3. Sharkov, E.A., 2009. *Breaking Ocean Waves: Geometry, Structure, and Remote Sensing*. Berlin, Heidelberg: Springer, 278 p. doi:10.1007/978-3-540-29828-1
4. Duncan, J.H., 1981. An Experimental Investigation of Breaking Waves Produced by a Towed Hydrofoil. *Proceedings of the Royal Society A: Mathematical, Physical and Engineering Sciences*, 377(1770), pp. 331-348. doi:10.1098/rspa.1981.0127
5. Phillips, O.M., 1985. Spectral and Statistical Properties of the Equilibrium Range in Wind-Generated Gravity Waves. *Journal of Fluid Mechanics*, 156, pp. 505-531. doi:10.1017/S0022112085002221
6. Phillips, O.M., 1988. Radar Returns from the Sea Surface—Bragg Scattering and Breaking Waves. *Journal of Physical Oceanography*, 18(8), pp. 1065-1074. doi:10.1175/1520-0485(1988)018<1065:RRFTSS>2.0.CO;2
7. Kudryavtsev, V.N., Hauser, D., Caudal, G. and Chapron, B., 2003. A Semiempirical Model of the Normalized Radar Cross-Section of the Sea Surface 1. Background Model. *Journal of Geophysical Research: Oceans*, 108(C3), 8054. doi:10.1029/2001JC001003
8. Korinenko, A.E., Malinovsky, V.V., Kudryavtsev, V.N. and Dulov, V.A., 2020. Statistical Characteristics of Wave Breakings and Their Relation with the Wind Waves' Energy Dissipation Based on the Field Measurements. *Physical Oceanography*, 27(5), pp. 472-488. doi:10.22449/1573-160X-2020-5-472-488
9. Korinenko, A.E., Malinovsky, V.V., Dulov, V.A. and Kudryavtsev, V.N., 2022. Estimation of the "Whitecap" Lifetime of Breaking Wave. *Fundamental and Applied Hydrophysics*, 15(1), pp. 61-72. doi:10.48612/fpg/5g5t-4mzd-94ab
10. Sharkov, E.A., 1994. [Experimental Investigations of Lifetimes for the Breaking Wave Disperse Zone]. *Izvestiya, Atmospheric and Oceanic Physics*, 30(6), pp. 844-847 (in Russian).
11. Bondur, V.G. and Sharkov, E.A., 1986. Statistical Characteristics of Linear Elements of Foam Formations on the Sea-Surface as Derived from Optical Sounding Data. *Issledovanie Zemli iz Kosmosa*, (4), pp. 21-31 (in Russian).
12. Callaghan, A.H., Deane, G.B. and Stokes, M.D., 2016 Laboratory Air-Entraining Breaking Waves: Imaging Visible Foam Signatures to Estimate Energy Dissipation. *Geophysical Research Letters*, 43(21), pp. 11320-11328. doi:10.1002/2016GL071226
13. Yurovsky, Y.Y., Kudryavtsev, V.N., Grodsky, S.A. and Chapron, B., 2021. Ka-Band Radar Cross-Section of Breaking Wind Waves. *Remote Sensing*, 13(10), 1929. doi:10.3390/rs13101929
14. Yurovsky, Y.Y., Kudryavtsev, V.N., Grodsky, S.A. and Chapron, B., 2023. On Doppler Shifts of Breaking Waves. *Remote Sensing*, 15(7), 1824. doi:10.3390/rs15071824
15. Fairall, C.W., Bradley, E.F., Hare, J.E., Grachev, A.A. and Edson, J.B., 2003. Bulk Parameterization of Air–Sea Fluxes: Updates and Verification for the COARE Algorithm. *Journal of Climate*, 16(4), pp. 571-591. doi:10.1175/1520-0442(2003)016<0571:BPOASF>2.0.CO;2
16. Mironov, A.S. and Dulov, V.A., 2008. Detection of Wave Breaking Using Sea Surface Video Records. *Measurement Science and Technology*, 19(1), 015405. doi:10.1088/0957-0233/19/1/015405
17. Kleiss, J.M. and Melville, W.K., 2010. Observations of Wave Breaking Kinematics in Fetch-Limited Seas. *Journal of Physical Oceanography*, 40(12), pp. 2575-2604. doi:10.1175/2010JPO4383.1

18. Kleiss, J.M. and Melville, W.K., 2011. The Analysis of Sea Surface Imagery for Whitecap Kinematics. *Journal of Atmospheric and Oceanic Technology*, 28(2), pp. 219-243. doi:10.1175/2010JTECHO744.1
19. Gemmrich, J.R., Banner, M.L. and Garrett, C., 2008. Spectrally Resolved Energy Dissipation Rate and Momentum Flux of Breaking Waves. *Journal of Physical Oceanography*, 38(6), pp. 1296-1312. doi:10.1175/2007JPO3762.1
20. Schwendeman, M.S. and Thomson, J., 2017. Sharp-Crested Breaking Surface Waves Observed from a Ship-Based Stereo Video System. *Journal of Physical Oceanography*, 47(4), pp. 775-792. doi:10.1175/JPO-D-16-0187.1
21. Phillips, O.M., Posner, F.L. and Hansen, J.P., 2001. High Range Resolution Radar Measurements of the Speed Distribution of Breaking Events in Wind-Generated Ocean Waves: Surface Impulse and Wave Energy Dissipation Rates. *Journal of Physical Oceanography*, 31(2), pp. 450-460. doi:10.1175/1520-0485(2001)031<0450:HRRRMO>2.0.CO;2

About the authors:

Alexandr E. Korinenko, Research Associate, Marine Hydrophysical Institute of RAS (2 Kapitanskaya Str., Sevastopol, 299011, Russian Federation), Ph.D. (Phys.-Math.), **Scopus Author ID: 23492523000**, **ORCID ID: 0000-0001-7452-8703**, **SPIN-code: 7288-8023**, korinenko.alex@mhi-ras.ru

Vladimir V. Malinovsky, Senior Research Associate, Marine Hydrophysical Institute of RAS (2 Kapitanskaya Str., Sevastopol, 299011, Russian Federation), Ph.D. (Phys.-Math.), **ORCID ID: 0000-0002-5799-454X**, **ResearcherID: F-8709-2014**, **SPIN-code: 9206-3020**, **Scopus Author ID: 23012976200**, vladimir.malinovsky@mhi-ras.ru

Contribution of the co-authors:

Aleksandr E. Korinenko – development of techniques and carrying out experimental studies, analysis and synthesis of the research results, preparation of the paper text

Vladimir V. Malinovsky – development of experimental research method, analysis and synthesis of research results, participation in the discussion of paper materials, preparation of the paper text

The authors have read and approved the final manuscript.

The authors declare that they have no conflict of interest.